Rev Argent Microbiol. 2019;51(3):268–277

asociación argentina de microbiología

REVISTA ARGENTINA DE MICROBIOLOGÍA

www.elsevier.es/ram

ORIGINAL ARTICLE

RNA-seq analysis of the response of plant-pathogenic oomycete *Phytophthora parasitica* to the fungicide dimethomorph

Kaiqiang Hao[a,c,1], **Beisen Lin**[b,d,1], **Fuzhao Nian**[a,1], **Xi Gao**[a], **Zhong Wei**[b], **Gang Luo**[b], **Yachun Lu**[b], **Mingxian Lan**[a], **Jinguang Yang**[c,*], **Guoxing Wu**[a,*]

[a] *State Key Laboratory for Conservation and Utilization of Bio-Resources in Yunnan, Yunnan Agricultural University, Kunming 650201, China*
[b] *Tobacco Science Research Institute of Baise Tobacco Company, Baise, Guangxi 533000, China*
[c] *Tobacco Research Institute of the Chinese Academy of Agricultural Sciences, Qingdao, Shandong 266101, China*
[d] *Hainan Provincial Branch of China National Tobacco Corporation, Haikou, Hainan, 571100, China*

Received 27 March 2018; accepted 26 August 2018
Available online 19 January 2019

KEYWORDS
Phytophthora parasitica;
Dimethomorph;
RNA-seq

Abstract *Phytophthora parasitica* is an important oomycete that causes disease in a variety of plants, dimethomorph fungicides being specific for oomycetes. The aim of this study was to use RNA-seq to rapidly discover the mechanism by which dimethomorph acts in the treatment of *P. parasitica*. We found that the expression of 832 genes changed significantly after the dimethomorph treatment, including 365 up-regulated genes and 467 down-regulated genes. According to the Gene Ontology (GO) enrichment analysis, pathway enrichment and verification test results, the following conclusions are obtained: (i) the treatment of *P. parasitica* with dimethomorph causes changes in the expression levels of genes associated with the cell wall and cell wall synthesis; (ii) dimethomorph treatment results in reduced permeability of the cell membrane and changes in the expression of certain transport-related proteins; (iii) dimethomorph treatment increased reactive oxygen species and reduced the expression of genes related to the control of oxidative stress.

* Corresponding authors.
E-mail addresses: yangjinguang@caas.cn (J. Yang), wugx1@163.com (G. Wu).
[1] These authors contributed equally to this work and should be considered co-first authors.

https://doi.org/10.1016/j.ram.2018.08.007

PALABRAS CLAVE
Phytophthora parasitica;
Dimetomorf;
RNA-seq

Análisis RNA-seq de la respuesta del oomiceto fitopatógeno *Phytophthora parasitica* al fungicida dimetomorf

Resumen *Phytophthora parasitica* es un importante oomiceto que origina enfermedades en una variedad de plantas; el fungicida dimetomorf es específico contra oomicetos. El objetivo de este estudio fue utilizar la tecnología de RNA-seq para descubrir rápidamente el mecanismo por el que el dimetomorf actúa en el tratamiento de *P. parasitica*. Descubrimos que la expresión de 832 genes se modificaba significativamente tras el tratamiento con dimetomorf, incluyendo 365 genes que son sobrerregulados y 467 genes que son subrregulados. El análisis de enriquecimiento de ontología de genes (GO), análisis de enriquecimiento de las vías y pruebas de verificación permitieron extraer las conclusiones siguientes: *1)* el tratamiento de *P. parasitica* con dimetomorf origina cambios en los niveles de expresión de los genes relacionados con la pared celular y su síntesis; *2)* el tratamiento con dimetomorf origina una reducción de la permeabilidad de la membrana celular, así como cambios en la expresión de ciertas proteínas relacionadas con el transporte, y *3)* el tratamiento con dimetomorf incrementó las especies reactivas del oxígeno y redujo la expresión de los genes relacionados con el control del estrés oxidativo.

Introduction

Phytophthora parasitica is a model oomycete plant pathogen[15]. *Phytophthora* represents a large group of devastating oomycete pathogens that causes important diseases in a wide variety of plant species, including potato, tomato, soybean, and valuable forest Trees[5,12]. These oomycete pathogens are a great threat to agricultural production and natural ecosystems[9,10]. For example, *Pytophthora infestans* causes late blight in potato and tomato, which resulted in the Irish famine in the 1840s and remains an uncontrollable disease[6].

The cell wall of *P. parasitica* mainly consists of 1-3-β-D glucans, 1-6-beta-D-glucans and cellulose[2], though the cell wall in fungi is primarily composed of chitin[13]. Most fungicides target chitin and sterol synthesis and are ineffective in controlling oomycete diseases. As the unique features of oomycetes and notably of *Phytophthora* confer insensitivity to most fungicides, a specific agent for control is required.

The carboxylic acid amide (CAA) fungicide dimethomorph is currently used to control *P. parasitica* var. *nicotianae*, *P. infestans* and *Plasmopara viticola* in China and remains an effective fungicide in controlling diseases caused by *P. parasitica* var. *nicotianae*[21].

According to wide-ranging investigations and mode of action studies, these agents have no effect on the respiration of pathogens and the biosynthesis of lipids, proteins and nucleic acids[7,10]. According to microscopic and ultrastructural studies investigating the destruction of the mycelial cell endometrial structure, dimethomorph may interfere with the formation of the cell wall of the pathogen[17].

Although only a few reports regarding the mode of action of dimethomorph are available, based on physiological and biochemical studies, we can investigate this topic using transcriptomics. Thus, we employed the *P. nicotianae* genome as a reference for a transcriptional study using Illumina RNA-seq[1,11]. We compared the transcriptional abundance between the control group and the processing group. This study provided new physiological insights into the mechanism of action of CAAs and provides a comprehensive illustration of the mechanism by which *P. parasitica* responds to the CAA-induced stress environment.

Methods and materials

Strain growth and processing conditions

P. parasitica was obtained from the Tobacco Research Institute of the Chinese Academy of Agricultural Sciences (Qingdao, China), stored at 4 °C and kept in the dark. In the dark, the experimental group (dimethomorph-treated) was exposed to 1.44 mg/l (lethal concentration 50, EC50) of dimethomorph in oat medium. *P. parasitica* grew over the entire Petri dish on the sixth day at 28 °C and was used as the initial experimental material. At the same time, the control group (control) was grown in a normal environment without pesticides and kept in the dark for six days. Then, the mycelia were collected. Three biological repetitions per treatment of dimethomorph-treated and control were performed.

RNA extraction, library construction, and sequencing

Total RNA was extracted with a Qiagen RNeasy Midi Kit using shredder columns from a Qiagen Plant RNeasy Kit following the manufacturer's instructions. Genomic DNA was removed using an on-column digestion with DNase (Qiagen) at twice the concentration recommended by the manufacturer. The concentration of the total RNA was

determined by spectrometry. Treatments and controls were repeated three times per group.

After extracting the total RNA, the eukaryotic mRNA was enriched by using oligo(dT) beads. Then, the enriched mRNA was fragmented into short fragments using a fragmentation buffer and reverse transcribed into cDNA using random primers. Then, the buffer, dNTPs, RNAse H and DNA polymerase I were added to synthesize the second-strand of cDNA. The cDNA fragments were purified with the QiaQuick PCR extraction kit and end repaired, poly(A) was added, and the fragments were ligated to Illumina sequencing adapters. The size of the ligation products was detected using agarose gel electrophoresis, and the products were PCR amplified and sequenced using Illumina HiSeq™ 2000 by Gene Denovo Biotechnology Co. (Guangzhou, China). The RNA-Seq data have been deposited in the NCBI Sequence (Short) Read Archive database with the SRA accession number SRP117995.

Read alignment of gene expression levels

The reads obtained from the sequencing included raw reads containing adapters or low-quality bases that would affect the subsequent assembly and analysis. Thus, to obtain high-quality clean reads, raw reads of FASTQ format were first processed through in-house Perl scripts, as follows: (1) reads containing adapters were removed; (2) reads containing more than 10% of unknown nucleotides (N) were removed; and (3) low-quality reads containing more than 50% of low quality (Q-value ≤ 10) bases were removed.

Analysis of differentially expressed genes (DEGs)

The edgeR package (http://www.r-project.org/) was used to identify the differentially expressed genes across the samples or groups. Genes with a fold change ≥ 2 and a false discovery rate (FDR) <0.05 were considered significant DEGs. The DEGs were then subjected to Gene Ontology (GO) functions and the Kyoto Encyclopedia of Genes and Genomes (KEGG) pathway enrichment analysis. (1) GO functional annotations of unigenes were obtained from Nr annotation results. GO annotations of unigenes were analyzed using the Blast2GO software.[4] Functional classification of unigenes was performed using WEGO software[24]. (2) Unigenes were aligned by BLASTx (evalue <0.00001) to protein databases in KEGG.

Quantitative real-time PCR (qRT-PCR) validations

Several differentially expressed genes were selected for qPCR analysis to determine whether the gene expression was consistent between the RNA-seq and qRT-PCR analyses. Total RNA was isolated using the TRIzol reagent according to the manufacturer's protocol, and the RNA was used for cDNA synthesis using reverse transcriptase. The S3a gene of *P. parasitica* was used as a housekeeping gene[8]. The 7500 Fast Real-time PCR System (Applied Biosystems, Foster, USA) was used to perform the thermocycling and record the changes in fluorescence. The quantification of each transcript was repeated using the total RNA as the starting material, qPCR runs were conducted using three technical replicates for each sample. The primers are listed in Table 1.

Detection of 1-3-β-D glucans content

We used the ELISA kit (Shanghai Jianglai's biological) to measure the content of 1-3-β-D glucans. The solid-phase antibody was prepared by coating the microtiter plate with purified 1-3-β-D glucans antibody. Samples were added to the microwells of the coated monoclonal antibody, and 1-3-β-D glucans were combined with specific antibodies (horseradish peroxidase-labeled, HRP-labeled). After thorough washing, 3,3′,5,5-tetramethylbenzidine (TMB) substrate was added to develop color. TMB was converted to blue under the catalysis of the HRP enzyme, finally turned yellow under the action of acid. The depth of color was positively correlated with 1-3-β-D glucans in the sample. The absorbance (OD) was measured with a microplate reader at a wavelength of 450 nm, and the concentration of 1-3-β-D glucans in the sample was calculated from a standard curve.

Detection of reactive oxygen species

The preparation of protoplasts is required for reactive oxygen detection; however, dimethomorph may interfere with the formation of the cell wall of the pathogen. Accordingly, this method cannot be used. ROS production was determined using a Reactive Oxygen Species Assay Kit (Beyotime). Briefly, after 6 d in normal culture, mycelium was collected and washed twice in warm PBS. Next, mycelium was added to medium containing 1.44 mg/l dimethomorph and pesticide-free medium for 1 h, followed by an incubation in prewarmed DCFH-DA at 37 °C for 20 min. Following two washes with PBS, reactive oxygen species in mycelium were measured at 488 nm/525 nm (excitation/emission) with a laser scanning confocal microscope (Leica).

Results

Data processing and analysis

Using the Illumina sequencing platform, the clean reads were harvested (data not shown) after performing quality control and filtering the data. In the following figures and tables in this paper, CK and HJ represent the control group, and the dimethomorph-treated group, respectively. After removing the contaminated and low-quality sequences (Table 2), all reads were mapped to the published genome, which contains 16 903 genes. In total, 16 867 and 16 888 genes were mapped for control and dimethomorph-treated groups, respectively. Unigenes represented by at least one mapped read were included in the subsequent analyses. The number of genes expressed in control and dimethomorph-treated accounted for 99.69%–99.81% of the total number of reference genes.

DEGs

To identify differentially expressed genes across dimethomorph-treated and control groups, the edgeR

Table 1 Oligonucleotide primers for qRT-PCR for DEG validation

Change	Gene name	Gene description	GO pathway	Forward primer (5′–3′)	Reverse primer (5′–3′)
	Unigene0002016	RxLR-like protein	GO:0043169; GO:0003824	CTACGGAACAAGCATCGC	TACACGGAGCCAAAGGAA
	Unigene0003097	Major facilitator superfamily domain-containing protein 7-b	GO:0044425;GO:0031224	TGGTGGCTTGTTACAGGCAGTT	GCTCGCTTGGATGGAGGAAA
Upregulated	Unigene0005650	Monoterpene epsilon-lactone hydrolase	GO:0003824	CTGTATCAACGCCTACGACT	GCAGCGACGGTATCTTCA
	Unigene0005891	T-complex protein 1, alpha subunit	GO:0005623;GO:0044464	AGCGTTCCCGTTGATTC	CCTTCCTGCTCCACCTTG
	Unigene0009353	TKL protein kinase	GO:0097367;GO:0036094	GGCTTCGTGAACGCAGTG	CTTCGCCGTATCCTCCTC
	Unigene0009796	Phytanoyl-CoA dioxygenase	GO:0016740y;GO:0016772	CTGAAACTGTGACGGAAGC	CGAGCGGTTGATTGGTAT
	Unigene0001184	Expansin-YoaJ	GO:0050896; GO:0043207	AGTTTGGTGGTGGTTCCTCT	GCTTTGGTCGGTCTGTGAT
Downregulated	Unigene0001431	Transmembrane protein	GO:0031224; GO:0016020	CAGCCAAAACACGAAGACCA	CGAACTTTTATTGAACAGGACAACC
	Unigene0013645	Beta-glucosidase btgE	GO:0003824; GO:0016787	GAACTGAATAGAGGAGTCGAGTGAA	TGGATGCGGTCTGGAATG
	Unigene0008035	Amine oxidase	GO:0003824; GO:0005488	CTCGATTTTGCCATCCAGGT	GTCGTTTAGTCATCTCGTTCTTCGT
	Unigene0000133	Acetylornithine aminotransferase	GO:0031224; GO:0044425	ATGCTCACCGCTTTCCTAACA	AACGCAGACCTCACAGACGA

Table 2 Control (CK) and dimethomorph-treated (HJ) (three biological replicates) raw read filters

Sample	Before filter reads num	After filter reads num (%)	Reads len	GC	Adapter (%)	Low quality (%)
CK-1	36006124	34 822 028 (96.71%)	150	56.98%	33 972 (0.09%)	1 150 082 (3.19%)
CK-2	27587172	26 756 694 (96.99%)	150	56.97%	19 476 (0.07%)	810 952 (2.94%)
CK-3	28289120	27 420 226 (96.93%)	150	56.80%	22 578 (0.08%)	846 276 (2.99%)
HJ-1	37833008	36 666 758 (96.92%)	150	56.37%	29 458 (0.08%)	1 136 742 (3%)
HJ-2	41538332	40 221 434 (96.83%)	150	56.61%	32 078 (0.08%)	1 284 744 (3.09%)
HJ-3	29881254	28 908 390 (96.74%)	150	56.45%	27 058 (0.09%)	945 774 (3.17%)

Table 3 Control (CK) vs. dimethomorph-treated (HJ) GO enrichment

	Description	GeneRatio[a]	BgRatio[b]	*p*-value	*q*-value	GO ID
	Intrinsic component of membrane	86 (65.65%)	1224 (39.11%)	0.000000	0.000000	GO:0016020
	Membrane	90 (68.7%)	1375 (43.93%)	0.000000	0.000000	GO:0044425
Cellular Component	Membrane part	86 (65.65%)	1298 (41.47%)	0.000000	0.000000	GO:0044425
	Cell periphery	6 (4.58%)	19 (0.61%)	0.000083	0.000901	GO:0071944
	External encapsulating structure	4 (3.05%)	7 (0.22%)	0.000093	0.000901	GO:0030312
	transporter activity	46 (14.38%)	548 (7.46%)	0.000010	0.001469	GO:0005215
	Phosphate ion transmembrane transporter activity	3 (0.94%)	3 (0.04%)	0.000082	0.006130	GO:0015114
	Oxidoreductase activity	35 (10.94%)	426 (5.8%)	0.000191	0.009356	GO:0016491
	Hydrolase activity acting on glycosyl bonds	21 (6.56%)	207 (2.82%)	0.000250	0.009356	GO:0016798
Molecular Function	Anion transmembrane transporter activity	12 (3.75%)	86 (1.17%)	0.000320	0.009561	GO:0008509
	Tetrapyrrole binding	10 (3.13%)	66 (0.9%)	0.000515	0.012822	GO:0046906
	Antioxidant activity	7 (2.19%)	35 (0.48%)	0.000654	0.013975	GO:0016209
	Transmembrane transporter activity	36 (11.25%)	484 (6.59%)	0.001024	0.019131	GO:0022857
	Organic acid transmembrane transporter activity	8 (2.5%)	51 (0.69%)	0.001473	0.019879	GO:0005342
	Organic anion transmembrane transporter activity	8 (2.5%)	51 (0.69%)	0.001473	0.019879	GO:0008514
	Multi-organism process	16 (5.33%)	66 (1.05%)	0.000000	0.000011	GO:0051704
	Phosphate ion transport	3 (1%)	3 (0.05%)	0.000108	0.01262	GO:0006817
	Single-organism process	163 (54.33%)	2785 (44.42%)	0.000260	0.020161	GO:0044699
	Response to stress	19 (6.33%)	169 (2.7%)	0.000416	0.024210	GO:0006950
Biological Process	Establishment of localization	70 (23.33%)	1045 (16.67%)	0.001440	0.044976	GO:0051234
	Single-organism localization	39 (13%)	508 (8.1%)	0.001908	0.044976	GO:1902578
	Hydrogen peroxide metabolic process	3 (1%)	6 (0.1%)	0.001947	0.044976	GO:0042743
	Cell wall organization	3 (1%)	6 (0.1%)	0.001947	0.044976	GO:0071555
	Single-organism transport	38 (12.67%)	492 (7.85%)	0.001961	0.044976	GO:0044765
	Nitrate metabolic process	2 (0.67%)	2 (0.03%)	0.002282	0.044976	GO:0042126

[a] Total number of differentially expressed genes (header figures), the number of differential genes annotated to a GO term, and the total number of differential gene percentages.
[b] Total number of all genes (header figures), the number of genes annotated to a GO term, and the percentage of total genes.

package (http://www.r-project.org/) was used. Based on comparison, we identified genes with a fold change $\geq$2 and a false discovery rate (FDR) <0.05 as significant DEGs. We found that the expression of 832 genes changed significantly after dimethomorph treatment, including 365 up-regulated genes and 467 down-regulated genes (Supplementary Table 1).

GO analysis of DEGs

Gene Ontology is a standardized system used for the functional classification of genes according to the 3 domains of biological process, cellular components, and molecular functions. To determine the functions of the differentially expressed genes in this study, all DEGs were annotated to the

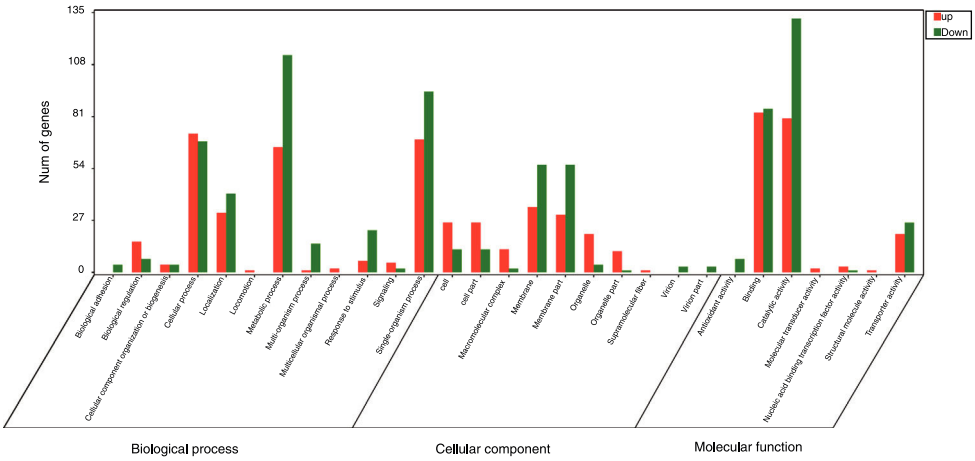

Figure 1 Inter-group difference enrichment analysis GO classification chart summary under dimethomorph treatment. The abscissa is the GO term, and the ordinate is the number of differential genes up- or down-counted. The histograms are based on three categories of biological processes, cellular components, and molecular functions, as well as up-and-down classification of differential genes.

Table 4 Control (CK) vs. dimethomorph-treated (HJ) pathway enrichment (the table below shows the results of the enrichment analysis of the pathway function. The meanings of the columns are similar to those of the GO function enrichment analysis)

Pathway	Candidate genes with pathway annotations (91)	All genes with pathway annotations (2756)	*p*-value	*q*-value	Pathway ID
Starch and sucrose metabolism	14 (15.38%)	99 (3.59%)	0.000003	0.000129	ko00500
Tyrosine metabolism	9 (9.89%)	40 (1.45%)	0.000004	0.000129	ko00350
Riboflavin metabolism	4 (4.4%)	16 (0.58%)	0.001493	0.034844	ko00740

terms in the GO database. Of the DEGs that were annotated in the GO database, 131 DEGs were annotated in cellular components, 320 DEGs were annotated in molecular functions and 300 DEGs were annotated in biological processes.

Of the 5 cellular components identified, the intrinsic component of the membrane (GO:0031224), the membrane (GO:0016020) and the membrane part (GO:0044425) were significantly enriched. Their proportions of total genes were 39.11%, 43.93% and 41.47%, respectively. Of the 17 molecular functions identified, transporter activity (GO:0005215), phosphate ion transmembrane transporter activity (GO:0015114) and oxidoreductase activity(GO:0016491) were significantly enriched, with total gene proportions of 7.46%, 0.04% and 5.8%, respectively. Of the 13 biological processes identified, multi-organism processes (GO:0051704), phosphate ion transport (GO:006817) and single-organism processes (GO:0044699); the number of these GO genes accounted for 1.05%, 0.05% and 44.42%, respectively, of the total genes (Table 3). These processes may be related to the treatment of *P. parasitica* with dimethomorph (Fig. 1).

KEGG analysis of DEGs

A KEGG pathway enrichment analysis was also performed to elucidate the interaction among dimethomorph-mediated pathways in stress responses. The DEGs in *P. parasitica* were matched to 70 different KEGG pathways. The most significantly altered pathways included starch and sucrose metabolism, tyrosine metabolism and riboflavin metabolism (Table 4, Fig. 2).

qRT-PCR validation

A qRT-PCR analysis was performed to validate the RNA-seq data of 11 genes (5 up-regulated and 6 down-regulated). As shown in Figure 3, the qRT-PCR data correlated well with the RNA-seq data ($R^2 = 0.7498$). Overall, the qRT-PCR data showed patterns that were similar to those obtained from the RNA-seq of these genes, although the particular values of the fold-change were different.

Detection of 1-3-beta-D-glucans content

In the determination of 1-3-beta-D-glucans using the ELISA test kit, we found that the content of 1-3-β-D glucans in *P. parasitica* decreased from 4.86 ± 0.22 pg/ml to 3.77 ± 0.49 pg/ml after treatment of dimethomorph ($F = 12.13 > F$ crit $0.05 = 7.708647$), The expression level of 1-3-β-D glucans changed significantly.

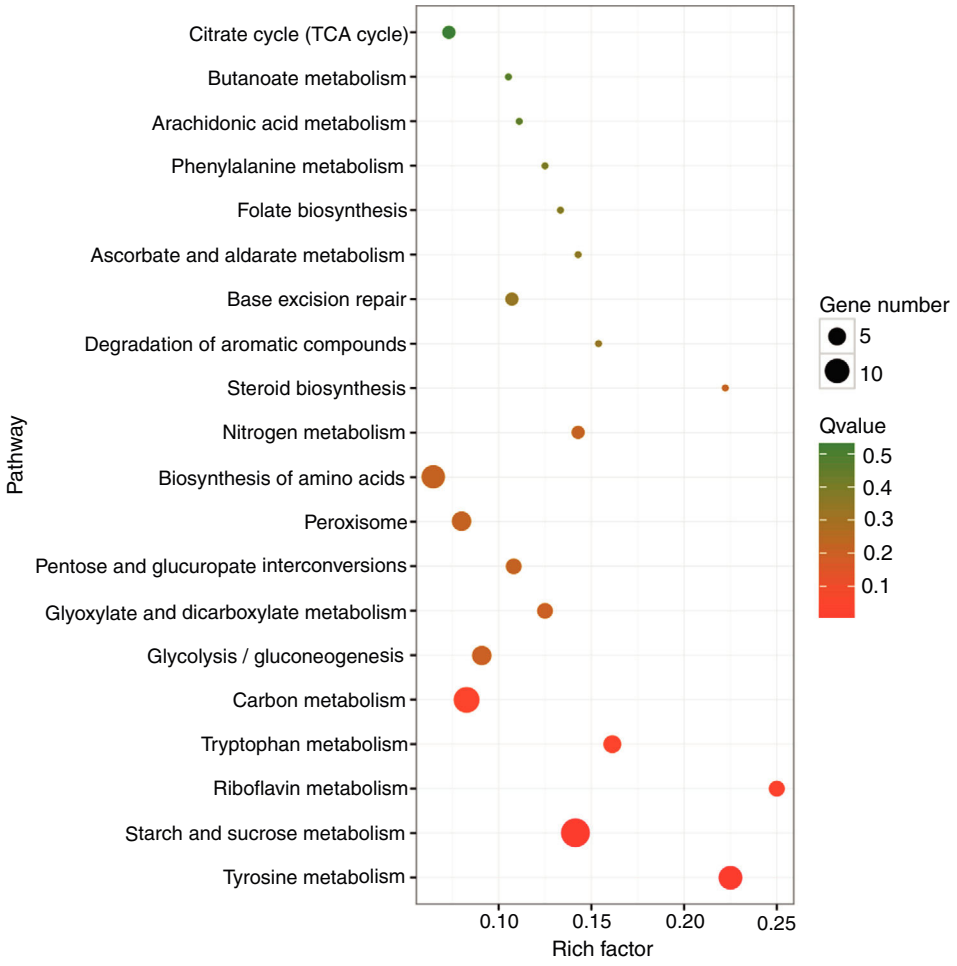

Figure 2 Top 20 enriched pathways (Rich Factor refers to the ratio of the number of genes located in the pathway entry in the differentially expressed genes to the total number of genes located in the pathway entry in all genes). The larger the Rich Factor, the higher the degree of enrichment.

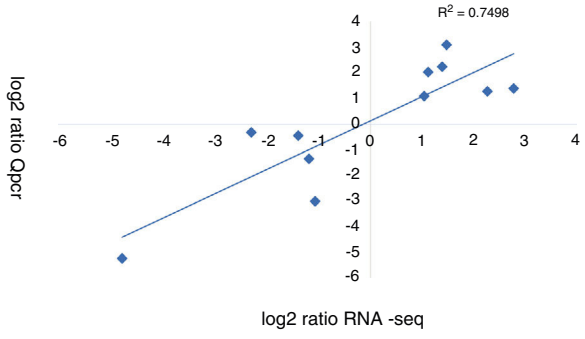

Figure 3 Comparison of log 2 ratios of RNA-seq and qRT-PCR for 11 genes. Treatment by dimethomorph 1 h (dimethomorph-treated), the same field of vision. The normal growth of mycelium (control), the same field of vision.

ROS content under different treatments

P. parasitica ROS levels after dimethomorph treatment for 1 h were much higher than those before treatment. Based on active oxygen area calculation, ROS levels increased up to 58% in response to dimethomorph treatment. In the normal growth environment, ROS levels were only 5% (Fig. 4).

Discussion

In this study, we analyzed the differential gene expression of *P. parasitica* after the exposure to a pesticide or under normal culture conditions. We found that 832 genes were significantly altered after the treatment with the acid morpholine, including 365 genes that were up-regulated and 467 genes that were down-regulated. Notably, GO and KEGG analyses of DEGs revealed significant differences, indicating that CAA has an impact on pathogens.

The effects of dimethomorph were systemic. Dimethomorph affects the formation of cellular and organelle membranes (the intrinsic components of the membranes, membrane parts), cell ion transport and transport protein formation (transporter activity, phosphate ion transmembrane transporter activity, phosphate ion transport) and affects the transport of exogenous substances (multi-organism process, single-organism process, oxidoreductase activity)[4,14].

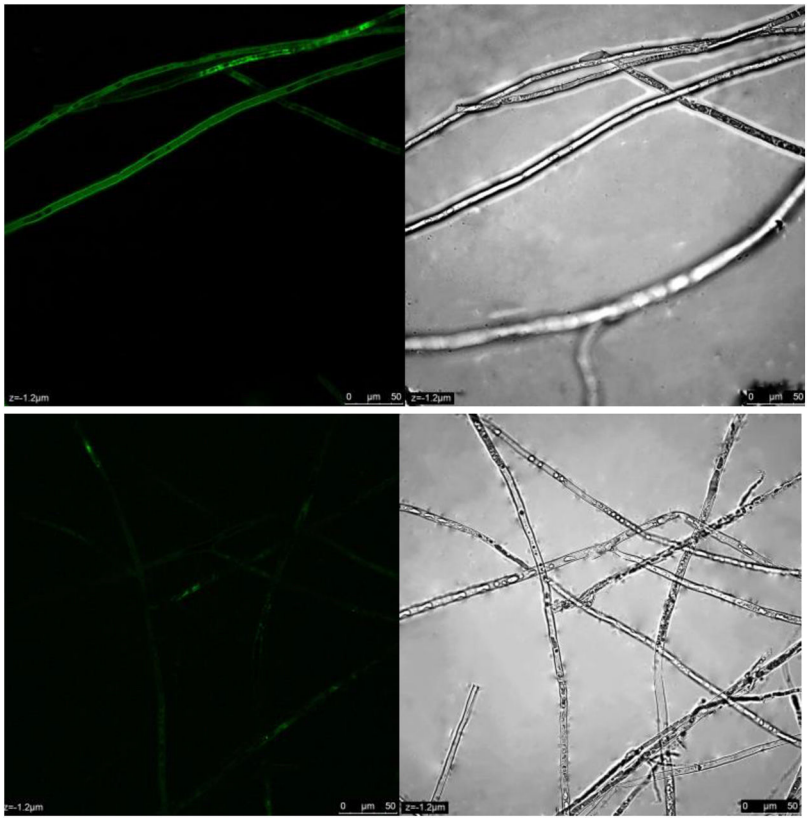

Figure 4 *Phytophthora parasitica* was measured at 488 nm/525 nm (excitation/emission) with a laser scanning confocal microscope (Leica). Green lights were ROS.

The cell wall and cell membrane are targeted by the CAA treatment

In this report, the RNA-seq results showed an altered expression of certain key genes in the cell membranes and cell walls that were strongly affected by dimethomorph. According to previous studies, the oomycete cell wall consists mainly of 1-3-β-D glucans and certain 1-4-β-D glucans and 1-6-β-D glucans[7,17].

The results of RNA-seq show that dimethomorph affects the synthesis of sugars involved in cell wall formation and the synthesis of cell membrane-associated proteins. Expression of 1,3-beta-glucan synthase (K00706), pectin esterase (K01051), glucan 1,3-beta-glucosidase (K01210) and beta-D-xyloidine 4 (K15920) was reduced (Supplementary Table 3, Supplementary Fig. 1). By the ELISA experiment, it was demonstrated that the treatment of dimethomorph had an effect on the formation of cell walls.

The cell wall structure is highly dynamic. The shape of the cell is strongly influenced by plasticity of the cell wall. Upon deposition, the cell wall polymers are integrated into existing structures and undergo extensive remodeling during cell expansion. These modifications involve a wide array of cell wall-modifying enzymes, such as the expansins, endoglucanases, polygalacturonases, peroxidases and various glycosidases that are localized to the cell wall or anchored in the plasma membrane of the cells. Several of these proteins have been identified in the cell walls of oomycetes[3,14].

Change in cell membrane structure and permeability

The fluid mosaic model is a hypothesis model of membrane structure. In this model, the proteins integral to the membrane include a heterogeneous set of globular molecules, each of which is arranged in an amphipathic structure with the ionic and highly polar groups protruding from the membrane into the aqueous phase and the nonpolar groups largely buried in the hydrophobic interior of the membrane[20]. Therefore, the structure and transport function of cell membranes are related to membrane proteins. Using RNA-seq, we showed changes in expression levels of several cell membrane structural proteins and transport-related proteins.

We obtained three cell membranes GO term through GO enrichment analysis, ''membrane'' (GO:0016020), ''intrinsic component of membrane'' (GO:0031224), and ''external encapsulating structure'' (GO:0030312). The last (GO: 0030312) is a term at a most detailed level, indicating that dimethomorph may affect cell membrane structural proteins (Supplementary Fig. 2).

The change in protein transport and transmembrane transport was that ''proteins related to phosphate transport'' were involved in ''phosphate ion transmembrane transporter activity'' (GO:0015114), ''anion transmembrane transporter activity'' (GO:0008509), ''transmembrane transporter activity'' (GO:0022857), ''organic acid transmembrane transporter activity''

(GO:0005342), and ''organic anion transmembrane transporter activity'' (GO:0008514). These changes affect the transport function of the cell membrane (Supplementary Fig. 3).

Increased reactive oxygen content

The production of reactive oxygen species (ROS) is an unavoidable consequence of aerobic metabolism. ROS include free radicals, such as superoxide anion ($O_2\bullet^-$) and hydroxyl radical (•OH), and non-radical molecules, such as hydrogen peroxide (H_2O_2) and singlet oxygen (O_2). The stepwise reduction in molecular oxygen (O_2) due to high-energy exposure or electron-transfer reactions leads to the production of ROS[19]. Environmental stresses, such as drought, salinity, chilling, metal toxicity, UV-B radiation, and pathogen attacks, lead to the enhanced generation of ROS due to the disruption of cellular homeostasis[18,22]. All ROS are extremely harmful to organisms at high concentrations. When the level of ROS exceeds the defence mechanisms, a cell is considered in a state of ''oxidative stress.'' The enhanced production of ROS during environmental stress can pose a threat to cells by causing peroxidation of lipids, oxidation of proteins, damage to nucleic acids, enzyme inhibition, and activation of programmed cell death (PCD) pathway, ultimately leading to the death of cells[16,23].

Dimethomorph is a type of environmental stress that can cause damage to the cell membrane. These injuries may substantially increase ROS. The oxidoreductase activity (GO:0016491), antioxidant activity (GO:0016209), and hydrogen peroxide metabolic processes (GO:0042743) were reduced, and all three ways reduced the control of ROS reduction. According to our experiments, dimethomorph treatment induced significant accumulation of ROS, which may cause apoptosis of *P. parasitica*.

Conclusions

In summary, we reported the effects of dimethomorph on *P. parasitica* using a dataset generated by de novo assembly of next generation sequencing data. These findings are valuable resources for future *P. parasitica* genomic studies and will also benefit researchers who study other closely related species of significant agricultural importance. The differentially expressed gene dataset will also provide useful candidate genes for the functional analysis of dimethomorph for the control of *P. parasitica*.

Conflict of interest

The authors declare that they have no conflicts of interest.

Appendix A. Supplementary data

Supplementary data associated with this article can be found, in the online version, at doi:10.1016/j.ram.2018.08.007.

References

1. Asmann YW, Michael B, Wallace E, Aubrey T. Transcriptome profiling using next-generation sequencing. Gastroenterology. 2008;135:1466–8.
2. Bartnicki-Garcia S. Cell wall chemistry, morphogenesis, and taxonomy of fungi. Ann Rev Microbiol. 1968;22:87–108.
3. Bouzenzana J, Pelosi L, Briolay A, Briolay J, Bulone V. Identification of the first Oomycete annexin as a (1→3)-β-D-glucan synthase activator. Mol Microbiol. 2006;62:552–65.
4. Conesa A, Götz S, García-Gómez JM, Terol J, Talón M, Robles M. Blast2GO: a universal tool for annotation, visualization and analysis in functional genomics research. Bioinformatics. 2005;21:3674–6.
5. Erwin DC, Ribeiro OK. Phytophthora diseases worldwide. American Phytopathological Society (APS Press); 1996.
6. Haas BJ, Kamoun S, Zody MC, Jiang RH, Handsaker RE, Cano LM, Bozkurt TO. Genome sequence and analysis of the Irish potato famine pathogen *Phytophthora infestans*. Nature. 2009;461:393.
7. Jackson KL, Yin J, Ji P. Sensitivity of *Phytophthora capsici* on vegetable crops in Georgia to mandipropamid, dimethomorph, and cyazofamid. Plant Dis. 2012;96:1337–42.
8. Judelson HS, Ah-Fong AM, Aux G, Avrova AO, Bruce C, Cakir C, Meijer HJ. Gene expression profiling during asexual development of the late blight pathogen *Phytophthora infestans* reveals a highly dynamic transcriptome. Mol Plant Microbe In. 2008;21:433–47.
9. Kamoun S, Furzer O, Jones JD, Judelson HS, Ali GS, Dalio RJ, Cahill D. The top 10 oomycete pathogens in molecular plant pathology. Mol Plant Pathol. 2015;16:413–34.
10. Kuhn PJ, Albert G, Loyness LE, Lee SA, Lindsley MC. Studies on the antifungal activity *in vitro* of dimethomorph, a novel fungicide active against downy mildews and *Phytophthora*. In: 9th international reinhardsbrunn symposium, modern fungicides and antifungal compounds. 1990. p. 229–38.
11. Kunjeti SG, Evans TA, Marsh AG, Gregory NF, Kunjeti S, Meyers BC, Donofrio NM. RNA-Seq reveals infection-related global gene changes in *Phytophthora phaseoli*, the causal agent of lima bean downy mildew. Mol Plant Pathol. 2012;13:454–66.
12. Kroon LP, Brouwer H, Cock AW, Govers F. The genus *Phytophthora anno* 2012. Phytopathology. 2012;102:348–64.
13. Latijnhouwers M, Wit PJ, Govers F. Oomycetes and fungi: similar weaponry to attack plants. Trends Microbiol. 2003;11:462–9.
14. Meijer HJ, Vondervoort PJ, Yin QY, Koster CG, Klis FM,Govers F, Groot PW. Identification of cell wall-associated proteins from Phytophthora ramorum. Mol Plant Microbe In. 2006;19:1348-58.
15. Meng Y, Zhang Q, Ding W, Shan W. *Phytophthora parasitica*: a model oomycete plant pathogen. Mycology. 2014;5:43–51.
16. Meriga B, Reddy BK, Rao KR, Reddy LA, Kishor PK. Aluminium-induced production of oxygen radicals, lipid peroxidation and DNA damage in seedlings of rice (*Oryza sativa*). J Plant Physiol. 2004;161:63.
17. Mitani S, Araki S, Yamaguchi T, Takii Y, Ohshima T, Matsuo N. Antifungal activity of the novel fungicide cyazofamid against *Phytophthora infestans* and other plant pathogenic fungi *in vitro*. Pestic Biochem Phys. 2001;70:92–9.
18. Mittler R, Oxidative stress. antioxidants and stress tolerance. Trends Plant Sci. 2002;7:405–10.
19. Sharma P, Jha AB, Dubey RS, Pessarakli M. Reactive oxygen species, oxidative damage, and antioxidative defense mechanism in plants under stressful conditions. J Bot. 2012:2012.
20. Simons K, Ikonen E. Functional rafts in cell membranes. Nature. 1997;387:569.
21. Sun H, Wang H, Stammler G, Ma J, Zhou M. Baseline sensitivity of populations of *Phytophthora capsici* from China to three carboxylic acid amide (CAA) fungicides and sequence

analysis of choline phosphotranferases from a CAA-sensitive isolate and CAA-resistant laboratory mutants. J Phytopathol. 2010;158:244–52.

22. Tanou G, Molassiotis A, Diamantidis G. Induction of reactive oxygen species and necrotic death-like destruction in strawberry leaves by salinity. Environ Exp Bot. 2009;65(2–3): 270–81.

23. Verma S, Dubey RS. Lead toxicity induces lipid peroxidation and alters the activities of antioxidant enzymes in growing rice plants. Plant Sci. 2003;164:645–55.

24. Ye J, Fang L, Zheng H, Zhang Y, Chen J, Zhang Z, Wang J. WEGO: a web tool for plotting GO annotations. Nucleic Acids Res. 2006;34 suppl_2. W293-7.